

Boundary Element Acoustics and the Fast Multipole Method (FMM)

Rajendra Gunda, Advanced Numerical Solutions, Hilliard, Ohio

Traditional Boundary Element Methods (BEM) for acoustic analysis have difficulty with large models and are thus limited to analysis of small bodies at low frequencies. Integration of the Fast Multipole Method (FMM) with BEM formulations leads to software programs with vastly superior performance.

Traditional BEM formulations result in fully populated system matrices, leading to large memory requirements and prohibitive analysis times. The FMM is an efficient way to compute the far field caused by a collection of acoustic sources. Integrating the FMM with BEM formulations leads to the development of next-generation, noise-analysis software programs with excellent performance. Just as the advent of the fast Fourier transform revolutionized digital signal processing, FMM has the potential to change the way we do acoustic simulations, due to its reduced computational complexity. FMM-BEM can handle ultra large-scale models (1 million unknowns and higher), allowing us to perform detailed system level noise analyses, and to extend BEM to the higher frequency regimes.

Current State of the Art

The flowchart in Figure 1 shows the virtual prototyping process widely followed in the industry for minimizing product noise and vibration levels. For instance, any automotive system must satisfy stringent noise, vibration and harshness (NVH) requirements while simultaneously meeting design goals for stress levels, durability and fatigue life, etc. A structural finite-element model that is built for stress analysis is typically used to provide the geometry and boundary condition inputs for an acoustic analysis. The conventional boundary element method (BEM) has some limitations that necessitate building a coarse BEM acoustic mesh.

Conventional BEM

The BEM technique is widely used to predict the sound radiation from vibrating structures, as it involves only surface discretization and solves exterior problems naturally. The key idea in BEM is to represent the acoustic field as a superposition of fields due to elementary (monopole, dipole) sources located on the radiator surface (Figure 2). The elementary solutions satisfy the Helmholtz equation exactly. The sound field from the vibrating structure must additionally satisfy the applied boundary condition, namely that the normal component of acoustic particle velocity must be equal to the structure velocity. The source strengths are adjusted to satisfy this kinematic continuity boundary condition.

Limitations of Conventional BEM

Size of the Computational Model. BEM influence matrices are fully populated, which limits the size of the models that can be analyzed. A 32-bit computer has 2 GB of addressable space for applications, limiting the largest BEM model to 11,585 unknowns, assuming in-core calculations. Out-of-core implementations reduce memory limitations at the expense of CPU time.

Upper Frequency Limit. Element size governs the maximum frequency to which a BEM model is valid. An empirical rule of six elements per wavelength (λ) is commonly used in the industry to avoid spatial aliasing (Figure 3). The number of elements (N) in a BEM mesh that is good to an upper frequency limit f_{\max} is given as:

$$N = N_x \cdot N_y = \frac{L_x}{(\lambda/6)} \cdot \frac{L_y}{(\lambda/6)} = \frac{36S}{\lambda^2} = \frac{36S}{c^2} f_{\max}^2 \quad (1)$$

Memory Usage = $O(N^2) = O(f_{\max}^4)$

Solution Time = $O(N^3) = O(f_{\max}^6)$

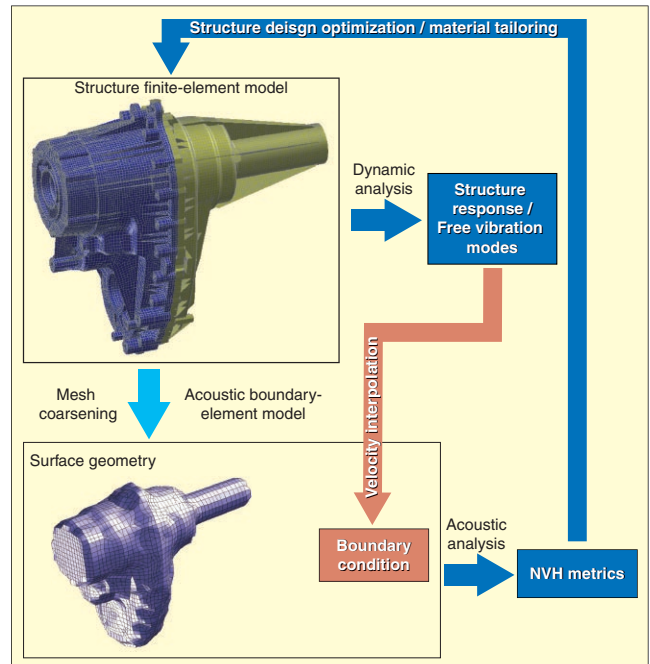


Figure 1. Virtual prototyping process for minimizing product NVH.

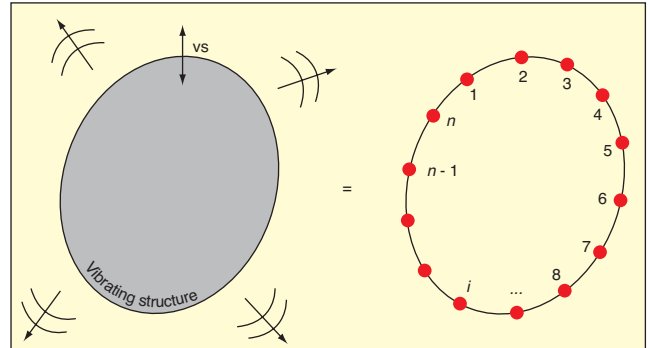


Figure 2. Sound field due to a vibrating structure represented as superposition of elementary solution, illustrating BEM concept.

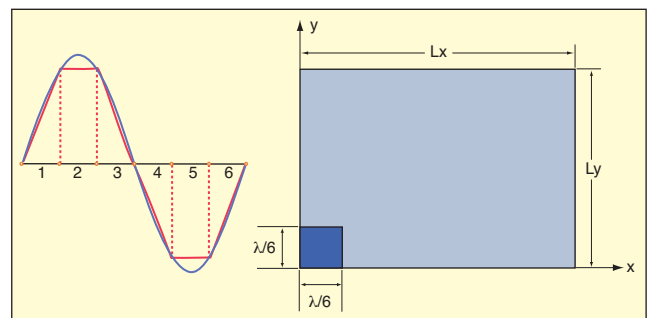


Figure 3. Minimum boundary element size required to avoid spatial aliasing (on the vibrating surface).

where N_x and N_y are the numbers of elements along two coordinate directions that define the radiator surface; S its surface area; O stands for “order of”; and c is the speed of sound in the fluid medium.

As expected, the number of elements is proportional to the

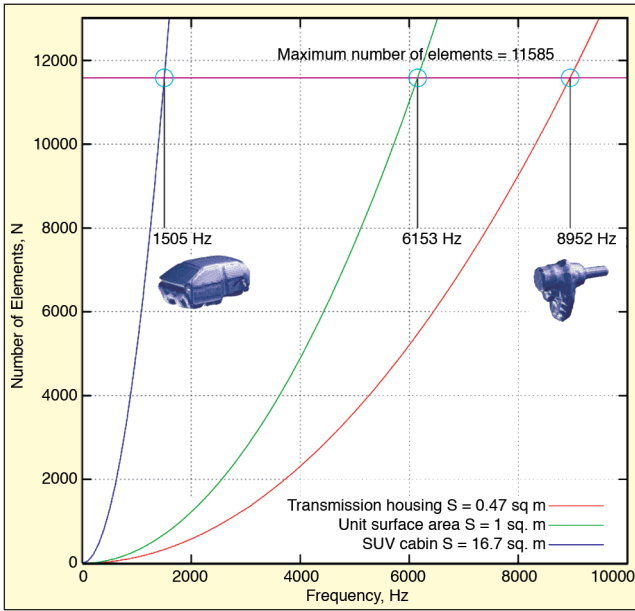


Figure 4. Maximum analysis frequency possible with conventional BEM. Conventional BEM is suitable for low-frequency analysis, primarily at component level.

radiator surface area S . However, the number of elements N is proportional to f_{\max}^2 , the square of the maximum analysis frequency. Doubling the frequency range of a BEM model requires a four-fold increase in the number of elements and a 16-time increase in RAM use. This adverse scaling law is the reason that conventional BEM is only suitable for a component level analysis and not for a full system analysis, as shown in Figure 4.

Coarsening Problems. Due to the model size limitations of conventional BEMs, the envelope of a structural finite-element mesh cannot be directly used for acoustic analysis. A mesh-coarsening process is adopted to produce an acoustic BEM mesh from the structure finite-element mesh (shown in Figure 1). Mesh coarsening increases the model preparation time and cost, and results in loss of geometrical features and reduces the frequency range for the BEM model. Mesh coarsening is only necessary due to the inability of conventional BEMs to handle large models. The mismatched structure and acoustic meshes also means that the vibration data from the dynamic structural analysis cannot be directly used for acoustic analysis. Instead, a time-consuming interpolation process is required to set up the acoustic boundary conditions. This situation can be remedied if acoustic BEM could be adapted to handle larger models.

Next Generation Code – Coustyx

To overcome the model size and frequency range limitations of conventional BEM, Advanced Numerical Solutions (ANSOL) has developed a new computational tool for acoustic analysis called Coustyx. Coustyx uses sophisticated BEM formulations in conjunction with FMM. Coustyx has an extensive selection of boundary condition options, and an intuitive graphical user interface. Multiprocessor support, pre/post processing, batch-mode option, and geometry/data transfer from standard-finite element analysis software are also available. Coustyx results are extensively validated against analytical solutions (for ideal radiators) and published experimental data on practical components or systems.¹ The examples used in this article are based on simulations performed using the Coustyx software.

Comparative Performance

We have performed benchmark studies to evaluate the performance of FMM-BEM relative to conventional BEM. The performance metrics compared were RAM use and total solution time. The problem of sound radiation from an oscillating sphere was considered due to the availability of an analytical solution. We constructed a number of sphere meshes with the total number of nodes ranging from 150 to 250,000. Figure 5 shows the results

from the benchmark study.

Figure 5 shows that FMM-BEM uses less memory and is faster than conventional BEM for all model sizes, and more so for larger models. BEM models with about 5,000 elements are typical in the industry. For such a problem, FMM-BEM is 13 times faster than conventional BEM and needs 1/3 as much RAM. The proposed FMM-BEM can handle much larger models (up to 1 million elements) that are impossible to analyze using conventional BEM (maximum 12,000 elements). The following sections describe how Coustyx delivers this “eye-popping” performance without any loss in accuracy.

New Formulations

Let $G(x,y)$ represent the sound pressure at a point x due to a unit point source located at y . The total sound pressure at x , due to n such sources of strength q_i (from Figure 2) are obtained by adding the individual source contributions:

$$p(x) = [G(x, y_1) \ G(x, y_2) \ \dots \ G(x, y_i) \ G(x, y_{n-1}) \ G(x, y_n)] \begin{Bmatrix} q_1 \\ q_2 \\ \vdots \\ q_i \\ q_{n-1} \\ q_n \end{Bmatrix} \quad (2)$$

The acoustic particle velocity vector $v(x)$ is related to the pressure gradient (∇p) as $v(x) = \nabla p(x) / i\rho_0\omega$, where ρ_0 is the ambient density of the fluid medium; ω is the angular frequency; and $i = \sqrt{-1}$ is the imaginary unit. The normal component (v_n) of the acoustic particle velocity at x is given by:

$$v_n(x) = \frac{1}{i\rho_0\omega} \left[\frac{\partial G(x, y_1)}{\partial n_x} \ \frac{\partial G(x, y_2)}{\partial n_x} \ \dots \ \frac{\partial G(x, y_i)}{\partial n_x} \ \frac{\partial G(x, y_{n-1})}{\partial n_x} \ \frac{\partial G(x, y_n)}{\partial n_x} \right] \begin{Bmatrix} q_1 \\ q_2 \\ \vdots \\ q_i \\ q_{n-1} \\ q_n \end{Bmatrix} \quad (3)$$

The kinematic continuity boundary condition must be satisfied at each boundary location y_i , leading to the following matrix equation for determining the source strengths $\{q\}$:

$$\{v_s\} = [A]\{q\} \quad (4)$$

In Eq. 4, $[A]$ is the BEM-influence matrix. Observe that $[A]$ is fully populated and has N^2 nonzero entries. The amount of computation required to build $[A]$ is proportional to N^2 , and solving Eq. 4 requires an additional $O(N^3)$ operation. The matrix $[A]$ is never explicitly constructed in Coustyx, and the source strengths $\{q\}$ are determined by solving Eq. 4 using iterative solvers such as GMRES (generalized minimum residual) that require only matrix-vector products.² This brings up the following question: How can we compute the matrix-vector product $[A]\{q\}$ when the matrix $[A]$ itself is not available? To answer this question, we have to go back to fundamentals and understand the physical meaning of $[A]\{q\}$.

By examining Eq. 4, it is clear each row of $[A]\{q\}$ represents the velocity response at a given source location due to the combined action of all the sources. Therefore, the matrix-vector product $[A]\{q\}$ is the velocity response at every source location caused by the whole ensemble of sources. We will take advantage of this fact in the development of a faster BEM code.

Fast Multipole Method

FMM is an efficient way to compute the far field caused by a collection of simple (monopole, dipole) sources. The main idea of FMM can be explained by considering the problem of computing the far-field response due to collection of simple sources clustered around a point O (Figure 6). Source strengths are denoted by q_i and d_i is the distance of a source from the cell center O . The cell size

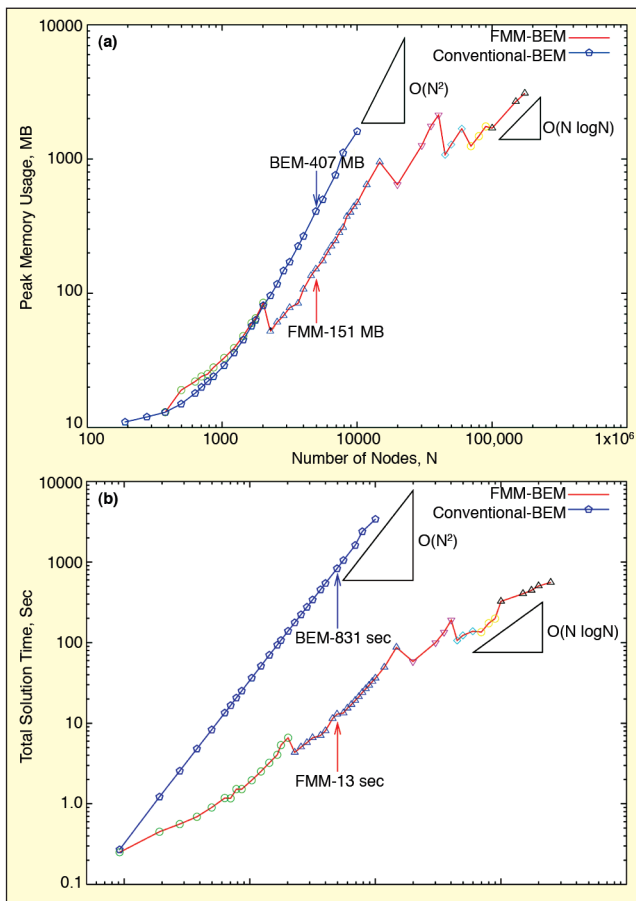


Figure 5. Performance of FMM-BEM (red) relative to conventional BEM (blue). Here N is the number of nodes in the boundary element mesh.

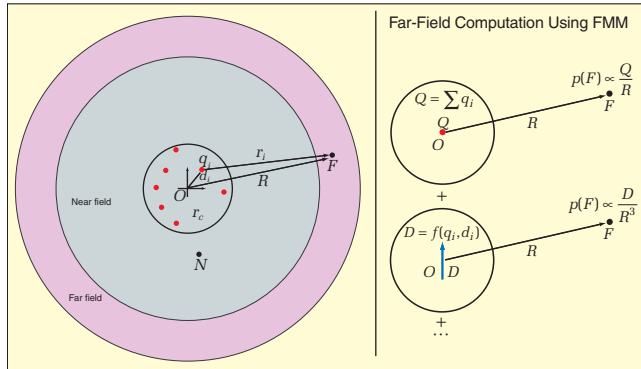


Figure 6. FMM concept – sound pressure at the far-field point F obtained by adding multiple source (Q, D) contributions.

is given as $r_c = \max(d_i)$. We are interested in computing the sound pressure at a far-field point F .

A naïve way to compute the sound pressure at F would be to add up the individual source contributions as shown in Figure 7a. FMM does the computation a bit differently (Figure 7b). A multipole expansion is performed about the cell center O (called the multipole expansion center), and the response at F is obtained by adding contributions of the multipole sources located at O . The advantage is that the contributions from higher-order multipole sources decay rapidly, and only a few terms are sufficient for an accurate calculation.³ The far field can then be computed accurately from the aggregate properties of the source distribution. Individual source locations and strengths are not very important for the field calculation at a remote observation point. This powerful idea has been used in a number of disciplines from gravitation to elasticity (Saint-Venant's principle⁴).

Far-field sound pressure $p(F)$ varies smoothly with distance R from the source cluster. Taylor series expansion is used to compute the sound pressure at points F_1, F_2 , etc., that are close to F .

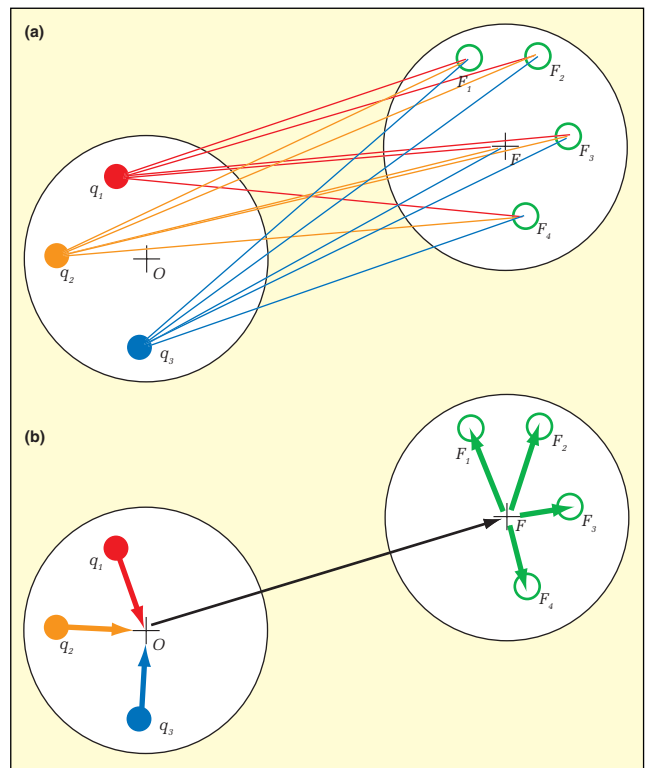


Figure 7. Far-field computation at observation points F , due to a collection of sources q .

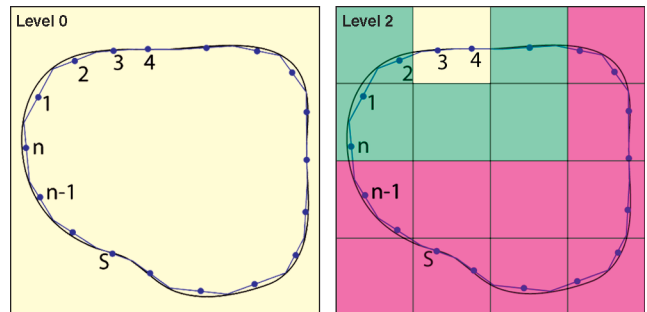


Figure 8. Single-level FMM for BEM surface sources.

The point F is called the local expansion center. Consider the mail delivery problem with n senders and m receivers, where O is a collection center, and F a distribution center. Organizing the calculations in this manner (Figure 7b) is very efficient, since the number of operations for n sources and m observation points reduces to $O(m+n)$ as opposed to $O(mn)$ for computing all the pair-wise interactions (Figure 7a), a huge benefit when m and n are large. Note that the near field does not offer any such simplifications and is computed in the usual way by adding the individual point source contributions.

Single-Level, Fast-Multipole Method

Eq. 4 shows that each row of matrix-vector product $[A]\{q\}$ represents the velocity response at a given source location due to the combined action of all the sources. The total velocity response at any observation point (say point 3 or 4 in Figure 8) has contributions from the near field (sources in the green region) and the far field (sources in the pink region). The contribution of the near-field sources is dominant given their proximity to the observation point, while the far-field sources provide the appropriate background level. The near field is computed directly, while the far field is computed effectively using FMM. To apply FMM for computing the far field, the BEM mesh is enclosed in a computational cube that is further subdivided into 64 smaller cubes (two-dimensional analogue shown in Figure 8). The sources contained within each Level 2 cube are aggregated to form a single equivalent multipole source at the cell center. The multipole source is used for the

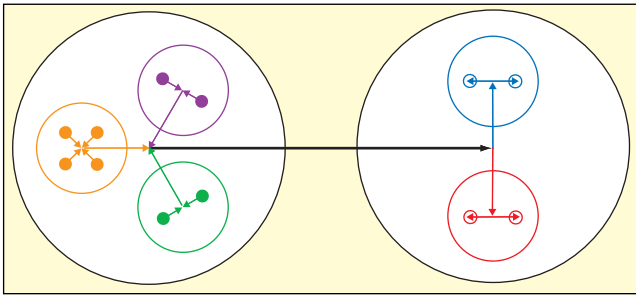


Figure 9. Sequence of calculations in Multilevel FMM. Solid circles represent acoustic sources; hollow circles represent observation points.

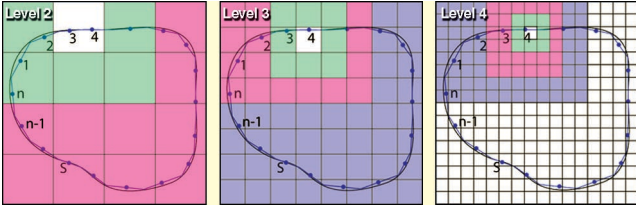


Figure 10. Multilevel FMM for BEM surface sources.

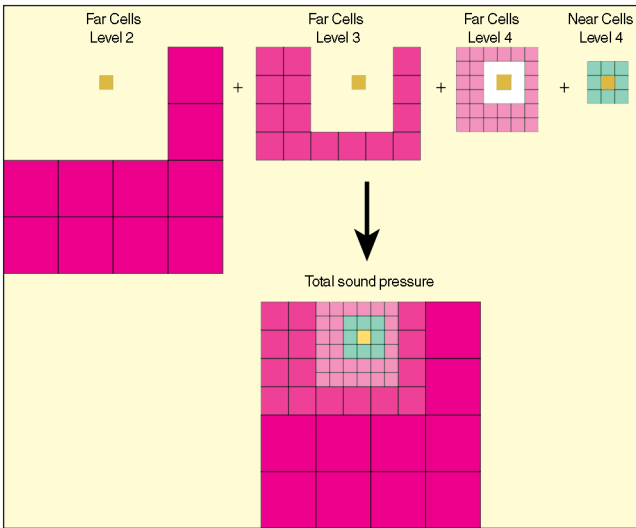


Figure 11. Downward pass in multilevel FMM.

response computation whenever an observation point is in its far field. Replacing the source-to-observation point interactions with cell-to-cell interactions results in significant speedup.

Multilevel Fast-Multipole Method

The main motivation for multilevel FMM is to maximize the portion of calculations that use FMM. The schematic in Figure 9 shows the sequence of calculations performed in multilevel FMM, where the solid circles represent acoustic sources, and the hollow circles represent observation points. The arrows represent how the acoustic sources are recursively aggregated to form multipole sources, which in turn are used for response computation at the observation points.

In multilevel FMM, a cell hierarchy is constructed by recursive subdivision of Level 2 cells (Figure 10). The cells adjacent to a given cell are called its neighbors. The cells at the next level that are obtained by subdividing a given cell are called its children. Interaction cells are cells at the same level that are not neighbors themselves, but whose parents are neighbors.

Two tree traversals are performed in multilevel FMM. The upward pass starts at the finest level (Level 4 in the example from Figure 10) and proceeds to the coarser levels. At Level 4, the sources contained within each cell are aggregated to form a single equivalent multipole source. At the next level (Level 3), the multipole sources from the children cell are combined. This process continues to Level 2. At the end of the upward pass, we have different sets of multipole sources whose expansions are valid

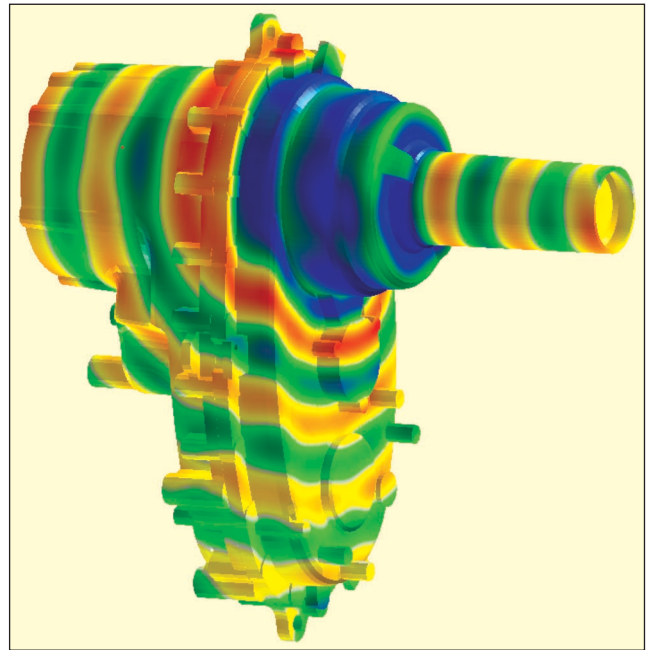


Figure 12. Sound pressure levels (in near field) radiated by an automotive transfer case at 5,000 Hz.

at varying spatial distances from the expansion centers.

The response computation is performed in a downward pass that starts at Level 2 and proceeds to the finest level, as illustrated in Figure 11 (for the observation point 4), using a multiscale approach that uses a coarse representation for the farthest cells and increasingly finer resolution as source cells get closer to the observation point.

Practical Applications

The following examples demonstrate the applicability of Coustyx to analyze complex noise and vibration problems in industry.

Example 1 – Radiation From Gearbox Casing. An automotive transfer case distributes the torque between the front and the rear axles. Noise radiation from the transfer case housing is an important factor affecting product quality. The BEM mesh considered for analysis⁵ was obtained by skinning the structure finite-element mesh. From Figure 12, it is clear that the transfer case BEM model has a high-fidelity representation of its surface geometry. Mesh coarsening and the associated approximations were completely avoided. The BEM Mesh has 44202 elements and 41288 nodes. The representative element length is about 7.8 mm, and the BEM model is valid up to 7255 Hz.

A surface velocity distribution induced by a spherical source located inside the transfer case was chosen as the boundary excitation, since it allows comparison with the exact analytical solution. Coustyx software allows functional representation for boundary conditions, making it very easy to implement this complex spatially and frequency-dependent boundary condition.

The surface sound pressure at 5 kHz shows the distinctive spherical spreading behavior that is in excellent agreement with the analytical solution. It was even possible to observe the quarter-wave modes of the bolt hole cavities.

Example 2 – Analysis of Transmission Assembly Noise. Noise analysis was performed on a system-level model of an automotive transmission that included gearbox housing, oil pan and transfer case. The structure mesh is extremely complex and includes solid elements, shell elements, re-entrant corners, and holes along with several rib stiffeners. The skinning algorithms in Coustyx automatically create a valid BEM model suitable for acoustic analysis – containing duplicate variable nodes along edge lines, constraint equations to handle surface junctions, and jump conditions at the free edges, all with minimal user input. The gearbox system model shown in Figure 13 has 2000 constraint equations, in addition to 40908 nodes and 48405 elements. Coustyx FMM-BEM solvers incorporate these junction constraints along with the BEM equations

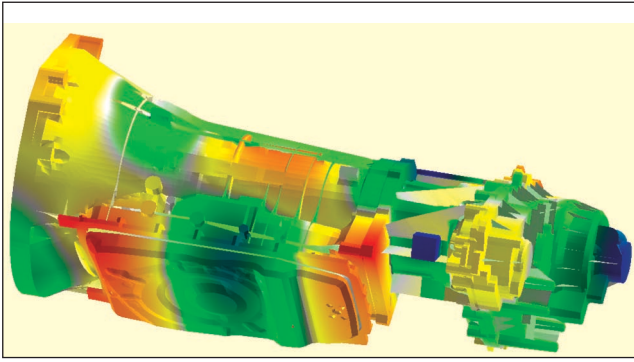


Figure 13. Contribution of surface panels to the noise radiation from a transmission assembly at 1 kHz.

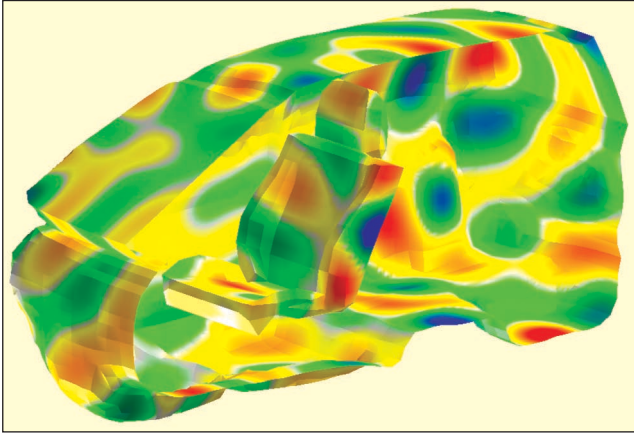


Figure 14. Noise levels inside a vehicle cabin at 1 kHz.

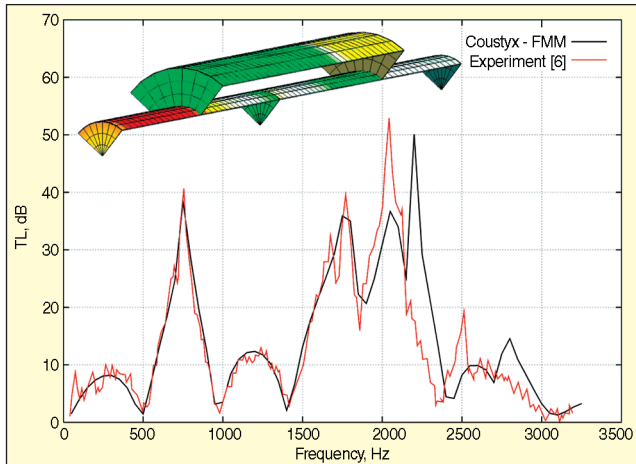


Figure 15. Transmission loss of a perforated muffler with flow plug.

to yield accurate solutions. Figure 13 depicts the contributions of various surface panels to the noise radiation at 1 kHz.

Example 3 – Vehicle Cabin Noise. Interior problems or noise prediction within enclosures has been difficult to handle in the past due to high modal density and the requirements for very fine BEM meshes to accurately capture high-frequency behavior. FMM-BEM techniques overcome both these limitations. The SUV cabin BEM model has 22836 elements and 22774 nodes. Figure 14 shows the sound pressure levels in an SUV cabin caused by a dashboard speaker at 1 kHz.

Example 4 – Transmission Loss of a Muffler. The transmission loss of a perforated muffler with a flow plug was computed in Coustyx (Figure 15). Coustyx has a perforated-plate boundary condition option that models the transfer impedance of a perforated plate as function of hole density. Taking advantage of symmetry, only a quarter model was analyzed. The transmission loss calculations from Coustyx analysis are in excellent agreement with published experimental results.⁶

Conclusions

Realistic simulation of full system models in the audible frequency range requires the integration of FMM with BEM, since FMM-BEM results in impressive performance improvements while retaining the solution accuracy. Next-generation software such as Coustyx, with integrated FMM-BEM, represent the way forward for acoustic simulations at the system level.

Acknowledgements

This material is based on work supported by the National Science Foundation under Grant No. 0548629. Any opinions, findings, conclusions or recommendations expressed in this material are those of the author and do not necessarily reflect the views of the NSF.

The author thanks Prof. Rajendra Singh and Sandeep Vijayakar for their encouragement and support, and Vijaya Ambarisha for performing the muffler transmission loss calculation that was used as an example in this article.

References

1. ANSOL website. <http://www.ansol.com/>
2. Van der Vorst, H. A., *Iterative Krylov Methods for Large Linear Systems*, Cambridge University Press, 2003.
3. Pierce, A. D., *Acoustics: An Introduction to its Physical Principles and Applications*, McGraw-Hill Book Company, 1981.
4. Greengard, L., *The Rapid Evolution of Potential Fields in Particle Systems*, Ph.D. thesis, Massachusetts Institute of Technology, 1987.
5. Gunda, R. and Vijayakar, S., "Acoustic Radiation from an Automotive Gear Box," SAE Paper Number 2007-01-2170.
6. Wu, T. W., *Boundary Element Acoustics – Fundamentals and Computer Codes*, WIT press, Southampton, Boston, pp.79-80, 2000.
7. Rokhlin, V., "Diagonal Forms of Translation Operators for the Helmholtz Equation in Three Dimensions," *Applied and Computational Harmonic Analysis*, Vol. 1, pp. 82-93, 1993.
8. Singh, R., (private communication), 2008. SV

The author can be reached at: rajendra.gunda@ansol.com.